Channel Models and Detectors for Two-Dimensional Magnetic Recording (TDMR)

Chan Kheong Sann[1], Rathnakumar Radhakrishnan[1], Kwaku Eason[1], Rachid Moulay Elidrissi[1], Jim Miles[2], Bane Vasic,[3] Anantha Raman Krishnan[3]

[1]Data Storage Institute (DSI), Agency for Science, Technology and Research (A*STAR), Singapore
[2]School of Computer Science, The University of Manchester, Oxford Road, Manchester M13 9PL, UK
[3]Department of Electrical and Computer Engineering, University of Arizona, Tuscon, Arizona, USA

***Abstract*— Two Dimensional Magnetic Recording (TDMR) is a novel recording architecture intended to support densities beyond those of conventional recording systems. The gains from TDMR come primarily from more powerful coding and signal processing algorithms that allow the bits to be squeezed more tightly on the disk, and yet be retrieved with acceptable error rates. In this paper we show the performance of several detectors over a pre-existing TDMR channel model. We also present some preliminary results for the next tier channel model based on micromagnetic simulations, coined the Grain Flipping Probability (GFP) model. This model requires a one-time computationally complex characterization phase, but subsequently provides fast and accurate 2D readback waveforms. Based on the granular channel model, we plot our results as a function of the channel bit size, normalized to the average grain size. This break from the norm of plotting the performance as a function of the Signal to Noise Ratio (SNR) yields several benefits that are discussed in the paper.**

***Index terms*—Two-dimensional magnetic recording (TDMR), 10 Tb/in^2, micromagnetic simulation, 2D channel detection, 2D channel models.**

I. Introduction

TDMR (Two-Dimensional Magnetic Recording) is a novel magnetic recording architecture proposed by Roger Wood [1] for densities towards 10Tb/in^2. The densities achievable via conventional means, are not expected to take the recording industry much beyond 1Tb/in^2. The *superparamagnetic limit* [2], [3] is going to slow and eventually halt areal density growth. In order to extend the life of magnetic recording, several novel system architectures are being proposed, which tackle the superparamagnetic limit from different sides. These architectures include Bit Patterned Media Recording (BPMR) [4], Energy Assisted Magnetic Recording (EAMR) which can be broken into Heat Assisted (HAMR) [5] and Microwave Assisted Magnetic Recording (MAMR) [6], and finally Two-Dimensional Magnetic Recording (TDMR) [1], [7].

A. Fundamental limits on magnetic recording

The superparamagnetic limit is fundamentally a trade-off between 3 competing parameters: the media Signal-to-Noise Ratio (SNR), the writeability of the media, and the thermal stability of the media. This trade-off is coined the *media trilemma*. As bit sizes are shrunk, one or more of the three necessarily gives way. In order to maximize the life of magnetic recording, all three parameters of the trilemma should be pushed to their limits.

BPMR approaches the trilemma by ordering the magnetic islands on the substrate. This accurate positioning of the magnetic islands (each island consisting either of a single grain, or a tightly coupled group of grains), maintains an adequate signal-to-noise ratio, with single-domain islands. The main challenge involves finding methods that permit mass-production of large areas of patterned media, cheaply. A second problem for BPMR arises in trying to read and write to ordered islands, in that the HDD system has to synchronize itself to the ordering of the islands on the media.

EAMR approaches the trilemma from the writeability/thermal stability trade-off. Without energy assisting, shrinking the grain-size will either require a large anisotropy to be stable (but the head can't flip the grains), or a small anisotropy to be writeable (but the grains will be thermally unstable, ie: spontaneously flip in time, due to vibrations from the ambient temperature). With EAMR, the anisotropy is designed to be large at ambient temperature ensuring thermal stability. During the write process, energy is injected (either through heat or microwaves) to excite the media, and reduce the magnetic field required to switch the grains. When the energy source is removed, the media returns to an unexcited, stable state.

TDMR approaches the trilemma from the SNR, and signal processing perspective. On the media, the channel bit cell is shrunk without proportionately reducing the grain-size. This will not put as much pressure on the writeability/thermal stability trade off, but instead will cause the SNR to fall below the levels needed by conventional 1D recording systems. Relying on more powerful, but more complex 2D coding and detection schemes, the aim of TDMR is to recreate the user-bits with an acceptable error level, from the lower SNR environment. TDMR's main challenges are in the coding and signal processing arena: to find the capacity limits, of a 2D granular media channel, and the codes and detectors that can approach those limits.

B. TDMR system considerations

Another challenge for TDMR stems from the writing method, which is known as shingled writing [8]. In order to

relax the requirements on the writing pole, a head that is larger than the track is assumed in the TDMR system. This permits sufficient head field, without the need for energy assist. To achieve narrower tracks, each sweep of the write head overlaps a certain percentage the previous track. Shingled writing may be used without two-dimensional readback at lower densities, however as the shingling gets more aggressive, the one-dimensional codes and detectors will eventually no longer be able to handle the interference coming from adjoining tracks. In 1D channels, inter-track interference (ITI) leads to a performance loss. With 2D channels, the ITI helps in making the decision for a given bit.

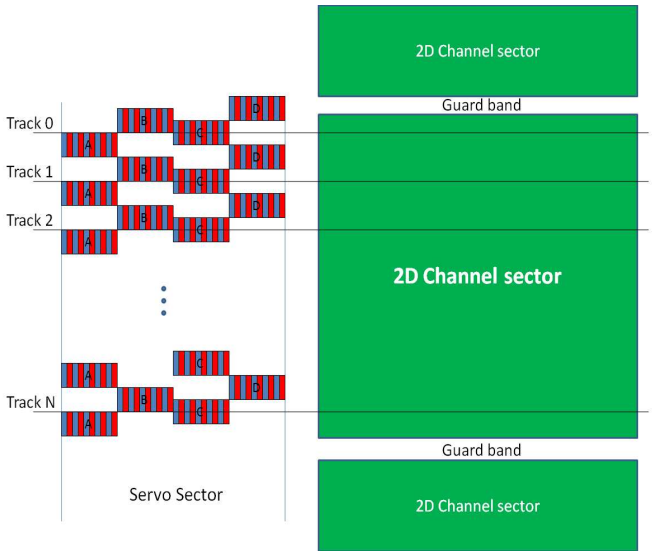

Fig. 1. A possible TDMR system setup using conventional ABCD servo that permits random access to the data.

A shingle-writing head would use the corner of the pole rather than the edge to write bits, and only that corner needs to have tight design specifications. Although shingled writing has advantages that permit wider heads to be used for writing narrower tracks, it causes some problems from a system-standpoint. Bits on future tracks get over-written by the larger head thus requiring careful design at the system level to permit updating of previously written data. To handle this, we propose a setup like the one shown in Figure 1.

In this setup, a 2D sector spans N tracks. Positioning of the head on the track is achieved with a conventional ABCD servo sector. As with today's recording systems, the entire sector of bits would be written at one go. We note that lag on write is not going to be problem as the operating system buffers the user data and the disk would write a track each revolution of the disk in the background. Lag on read however could cause unacceptable delays to the user. Each 2D sector would be updated independently of adjoining 2D sectors due to the guard band. The choice of the 2D sector size is a design trade off between more density gain from 2D coding and signal processing for larger sectors, versus shorter readback lags and smaller minimum file sizes for smaller sectors. A first trial system could consist of a 2D sector of 8 tracks having 4096 bits each. This would conveniently align with the 4096 kbyte standardization effort being pushed by IDEMA, while retaining the familiar 512 bytes in the downtrack dimension, with possible re-use of the existing codes in that dimension. It is of interest to note that track N is never overwritten, and thus the signal from that track will have a higher SNR than any other track in the 2D sector.

Other system-level changes could help to improve the performance of a TDMR drive. Having multiple readers mounted on the same slider could pick off the 2D sector in fewer revolutions, while writing large files onto 2D sectors spanning the same set of tracks would read off different parts of the file during the entire revolution instead of only during a small part of the revolution.

In [7], a preliminary TDMR simulation system is proposed and some basic detectors are tested with media proposed there. In this work we show the results from additional 2D detectors that are implemented on the same Voronoi grained channel model in [7]. We also show some preliminary results in the development of the third tier model based on micromagnetic simulations mentioned in [7].

II. The Grain Flipping Probability (GFP) Model

The model in [7] was based on Voronoi cells mimicking the geometry of the grains on the media. In that model each grain was written by the bit that covered the grains' Voronoi nucleus. In this paper we use the same Voronoi cell geometry, but propose a more realistic model to determine which grains should be flipped, based on micromagnetic simulations [9]. Micromagnetic simulations are a much more time-consuming but accurate way of modeling the evolution of the magnetization of particles with time in the presence of a field. Here we propose to use micromagnetic simulations to populate a look-up table (LUT) of probabilities that tell how likely a grain is to flip in a given set of circumstances per bit interval. Using the LUT to determine which grains flip, results in more realistic simulations during system performance evalution, while not having to pay the unacceptable delays in running micromagnetic simulations, except during the initial phase of characterizing the LUT. We have coined this the Grain Flipping Probability (GFP) model.

The process of characterizing and using the LUT is as follows. Firstly tensor and grain statistic information need to be generated and computed for the Voronoi media geometry. Next, given a head field, micromagnetic simulations are run on the media using the previously computed data for a range of bit patterns, yielding granular magnetizations such as shown in Figure 2. Statistics from each simulation are used to characterize the probabilities in a multi-dimensional LUT that has a dimension for each parameter deemed significant in influencing the probability of flipping. Choice of these parameters is critical, and we have selected them in order of greatest influence on the probabilities. Parameters are chosen that vary on a bit-to-bit or on a grain-to-grain basis. Too few parameters will result in an ineffective LUT, while too many parameters will result in a LUT that takes too long to adequately characterize. Once the LUT is characterized, the final phase is to use those probabilities to quickly flip

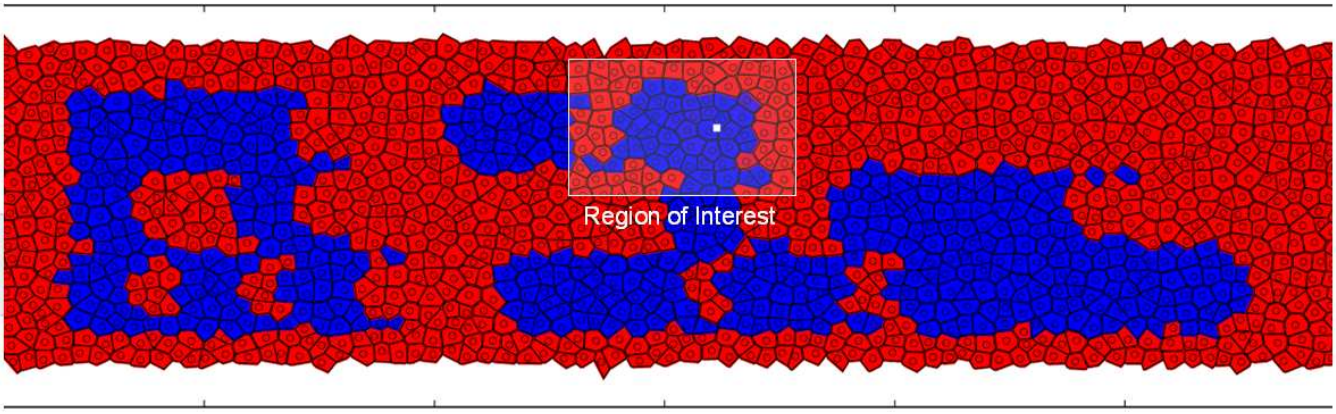

Fig. 2. Grain magnetizations at the output of the micromagnetic simulation. Red grains are positively magnetized while blue are negative. Current head location is marked by the white square and the region of interest surrounds those grains possibly influenced by the write head.

grains using a random number generator (RNG) in channel simulations to mass-produce accurate granular magnetizations, and thus 2D readback waveforms to simulate the channel. Here we describe the characterization process of the GFP model in more detail.

A. GFP model characterization

Figure 2 shows the results of a micromagnetic simulation run on a rectangular media with 2000 grains and with nominal values of $M_s = 250$ kA/m, $K_1 = 105$ kJ/m^3 and $H_k = 668.5$ kA/m. The head field was the same as the one used in [1] and [7]. An array of bits was written onto the media with a small shingle overlap. The density of the characterized model is valid only at the density of the simulations at which the model was characterized, and determined by the parameters of the micromagnetic simulation. New micromagnetic simulations need to be run at each density (shingle overlap/write clock frequency) of interest.

A region of interest (ROI) is defined about each nominal bit location, shown in the example of Figure 2. The ROI needs to be large enough to capture those grains around the head that have a non-zero probability of flipping, in the current bit interval (i.e. the duration of writing one bit). Every grain in the ROI has a probability of flipping conditioned on a large number of parameters. In the first trial, we choose 4 of them for inclusion in the LUT. The first 2 parameters are the location (x and y) of the grain center relative to an arbitrarily chosen origin attached to the head. They are discretized into 12 bins each. The next parameter is the anisotropy constant of the grain H_k discretized into 8 bins. As we will want to characterize the LUT for media with a switching field distribution (varying H_k), this parameter will need to be considered on a per-grain basis. The last parameter considered is the surrounding bit pattern, discretized into 16 bins (4 bit combinations). The 4 bits playing a role in the LUT are: the current bit, the previous bit on the current track, the bit at the same position as the current bit on the previous track, and the previous bit on the previous track. The current bit's magnetization is obviously going to have the largest degree of influence on whether grains in the ROI flip or not. The other abovementioned bits determine magnetizations of grains in the vicinity of the ROI, and these nearby grains have an effect on the probability of grains in the ROI flipping, through the exchange, and demag fields. Ideally we would like to include the influence of the entire past bit history, but this would be computationally infeasible.

These 4 parameters yield a total of 18432 bins along 4 dimensions of the LUT that need to be filled with enough data to give sufficiently accurate statistics. The LUT itself is stored as two 4-dimensional arrays: the numerator and denominator arrays. The denominator array keeps a count of the grains in each condition (determined by the state of the parameters) that *could* flip at the end of each bit-interval. This is a count of the grains within the ROI that are opposite in magnetization to the applied field. The numerator array keeps a count of the grains that *do* flip at the end of each bit interval. The probability of flipping in a given bit-interval is obtained by dividing the two arrays. In the first trial characterization, 200 sectors of micromagnetic simulations (of 60 bits in 3 rows each) were run in parallel on 24 cores taking over 1 day and giving 372832 samples in the denominator and 193852 samples in the numerator, or an average of about 20 samples per bin. One should take into consideration that not all bins are equally used, nor equally useful.

While it is not possible to view a 4-dimensional LUT, the numerator and denominator can be summed over any dimension and the resulting arrays divided to arrive at lower dimensional probability tables as a function of the remaining dimension's parameters. For example, summing over the H_k and bit pattern bins leave the probability as a function of the x and y bins. This gives a probability distribution as a function of the grain position within the ROI or a probability footprint. It is shown in Figure 3 for three cases: summing over bit patterns where the current bit is a plus, summing over bit patterns where the current bit is a minus and summing over both.

The probability footprints have captured an assymetry in the micromagnetic simulations that arises due to the positively magnetized DC background that make it easier to write a negative bit than a positive one via the demag field. Another feature of the plots is that they are not the usual crescent

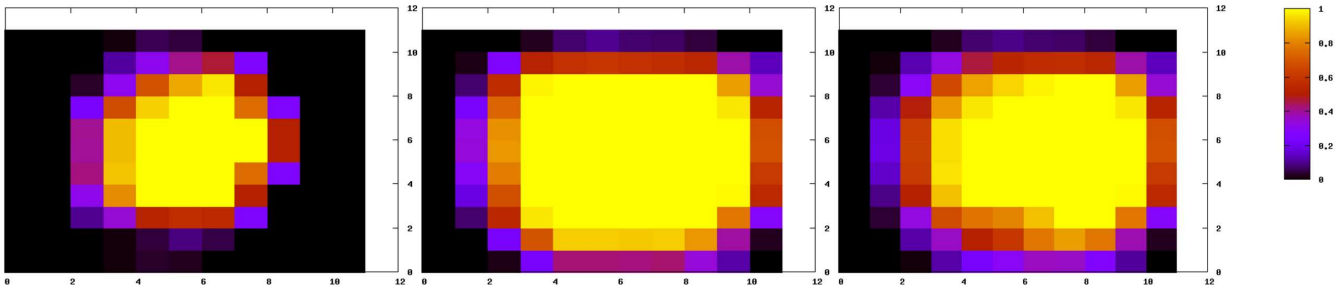

Fig. 3. Probability footprint for a. current bit plus (left) b. current bit minus (middle) c. both plus and minus (right)

shaped footprints that one might expect. This is because the crescent shape is due to the future bit partially over-writing the leading edge of the current bit. The probability model does not take into account any effects caused by future bits, only the past and current bits are accounted for.

III. 2D Detectors

Since TDMR was first proposed by Wood et. al. [1], the focus of investigation has been to identify the operating point that maximizes the user storage capacity. We provide some insight into this problem through simulations. Specifically, we determine the performance of various 1-D and 2-D detectors on the TDMR channel using the Voronoi model, and draw some conclusions on the achievable channel densities.

The need for 2-D detection is not unique to TDMR systems. It is a vital component of optical storage systems, image processing and wireless communications. As a result, there has been considerable work devoted to developing 2-D detectors in the recent past. See [10] for a survey of various 2-D detectors. However, it is still largely an open problem as practical detectors that are close to optimality are still elusive. In this section, we discuss various 1-D and 2-D sub-optimal detectors that are applied to the TDMR system.

A. Inversion Detector

The inversion detector (or zero-forcing equalizer) is a well-known detection technique for one-dimensional magnetic recording systems. It is known to result in inferior performance compared to partial response equalization techniques because of noise enhancement. However, from the discussion in the previous section, it is clear that the noise in TDMR systems consists predominantly of media noise, making the additive electronic noise insignificant. Consequently, it is worth exploring the applicability of the inversion detector to TDMR, especially at ultra-high densities. In [11], some reasonable error rate performance was reported for the case when the media was modeled as a perturbation of Voronoi-based square lattice.

If the binary input of the TDMR system is denoted as $A = \{a_{i,j}\}_{n\times n}$, and if the corresponding magnetization of the medium be denoted as $m(t_1, t_2)$, then the readback output $R = \{r_{i,j}\}$ is given as,

$$r_{i,j} = \iint h(\tau_1, \tau_2) m(i - \tau_1, j - \tau_2)\, \mathrm{d}\tau_1\, \mathrm{d}\tau_2$$

where, $h(\tau_1, \tau_2)$ is the impulse response of the system. If the magnetization pattern is ideal, the sampled readback output can be written as the following discrete convolution,

$$r_{i,j} = \sum_{k_1} \sum_{k_2} h_{k_1,k_2} x_{i-k_1, j-k_2}$$

where,

$$h_{k_1,k_2} = \iint_{A_{k_1,k_2}} h(\tau_1, \tau_2)\, \mathrm{d}\tau_1\, \mathrm{d}\tau_2,$$

and $A_{i,j}$ is the region spanning the $(i,j)^{th}$ bit cell. Representing the $n \times n$ 2-D input and output matrices as n^2 1-D vectors, the ideal output can be written as a product of matrices, $\bar{R} = \hat{H}\bar{X}$, where $\hat{H}$ is a $n^2 \times n^2$ matrix. Since at the receiver there is no knowledge of the irregularity, the inversion detector assumes perfect magnetization and determines $\bar{X}$ from the polarity of $\hat{H}^{-1}\bar{R}$.

B. 2-D MAP Detector

For the TDMR system, the optimal detector is the one that maximizes the bit *a posteriori* probability (MAP) $p(a_{i,j}/R)$. However, the noise coloration and two-dimensional ISI makes it almost impossible to design such a detector. As a result, we focus on the application of practical, but sub-optimal detection schemes. Almost all such techniques first require the least-mean square linear characterization of the TDMR channel as discussed in the previous section, whereby, the channel output can be written as,

$$\begin{aligned} r_{i,j} &= \iint h(\tau_1, \tau_2) m(iT_1 - \tau_1, jT_2 - \tau_2)\, \mathrm{d}\tau_1\, \mathrm{d}\tau_2 \\ &= \sum_{\lambda_1 = -L_r/2}^{L_r/2} \sum_{\lambda_2 = -L_c/2}^{L_c/2} \tilde{h}_{\lambda_1,\lambda_2} a_{i-\lambda_1, j-\lambda_2} + e_{i,j} \end{aligned}$$

where, T_1 and T_2 are the sampling period in the two dimensions and $\tilde{h}$ is the characterized channel of size $L_r \times L_c$. In this paper, we do not consider the effects of noise coloration. With the assumption that the noise samples $e_{i,j}$ are independent and Gaussian distributed, the MAP detector can be implemented using the BCJR algorithm that operates on the trellis of the 2-D ISI channel. However, it is still prohibitively complex even for modest sector sizes. If a sector comprises of M rows, then the 2-D trellis will have $2^{M\cdot(L-1)}$ states and 2^M incoming and outgoing branches for each state.

MAP detectors for 2-D ISI channel with independent and identically distributed noise has received considerable attention since the multi-head multi-track magnetic recording system was first proposed by Barbosa [12]. Since then, many sub-optimal and relatively low-complex algorithms have been proposed. A popular and recurring theme has been to divide the sector into many smaller sets of rows (or columns) and detect each set independently. On one extreme, every row of the sector can be independently detected by ignoring the ITI. On the other extreme, all rows of the sector can be jointly detected. Naturally, many architectures are possible in between these two extremes with varying levels of complexity and sub-optimality [10]. In this work, we focus on the performance of the detection schemes that form the two extremes. We also focus on an another approach that was recently proposed in [13], which we discuss next.

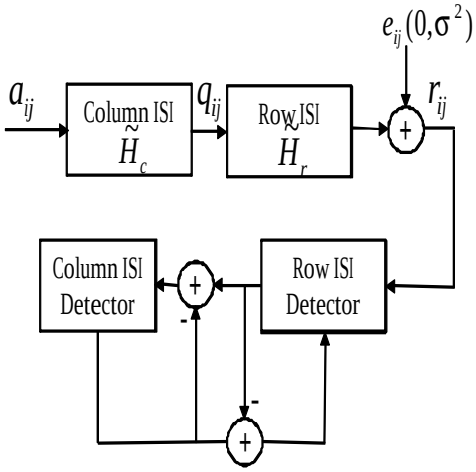

Fig. 4. Iterative detection for a separable 2-D ISI channel.

C. Separable 2-D MAP Detector

In [13], it was shown that if the 2-D ISI matrix is separable into a row and a column vector, then a relatively low-complex detector can be developed. To see this, consider the 2-D ISI matrix $H = \{h_{i,j}\}$. If $H = \bar{U}\bar{V}$ where, $\bar{U}$ and $\bar{V}$ are column and row vectors, respectively then the output of such a channel is given as,

$$\begin{aligned} r_{i,j} &= \sum_{t_1}\sum_{t_2} h_{i-t_1,j-t_2} a_{t_1,t_2} \\ &= \sum_{t_1}\sum_{t_2} u_{i-t_1} v_{j-t_2} a_{t_1,t_2} \\ &= \sum_{t_1} u_{i-t_1} \left(\bar{V} * a_{t_1,:}\right) \\ &= \sum_{t_2} v_{j-t_1} \left(\bar{U} * a_{:,t_2}\right) \end{aligned}$$

where, $'*'$ denotes the convolution operation, $a_{t_1,:}$ and $a_{:,t_2}$ denote row t_1 and column t_2 of matrix A, respectively. Therefore, if the readback response is separable, then the channel can be considered to be a concatenation of two 1-D channels, one resulting in ISI along the downtrack direction (row) and the other resulting in ISI along the cross-track direction (column). Consequently, an iterative detector consisting of two 1-D detectors can be developed as shown in Fig. 4. The row-ISI detector is a non-binary MAP detector, whereas the column-ISI detector is a binary MAP detector, which does not use channel information. The extrinsic information produced by the two detectors are used as *a priori* probabilities by each other in subsequent iterations. More details of the algorithm can be found in [13].

The linear channel response that best characterizes the TDMR channel may not be separable. However, usually some small approximations are often enough to make them separable. In this work, since we assume a bit aspect ratio (BAR) of 2, the ISI is dominant over ITI and as a result we choose to approximate the ITI in order to achieve separability. For a 3×3 characterized channel matrix $\tilde{H} = \{\tilde{h}_{i,j}\}_{3\times 3}$, the separable vector components are given as,

$$\begin{aligned} v_i &= \tilde{h}_{2,i} \ \forall \ i = \{1,2,3\}, \\ u_i &= \frac{1}{3}\sum_j \frac{h_{i,j}}{h_{2,j}} \ \forall \ i = \{1,2,3\}. \end{aligned}$$

The bottle-neck in this detector is the complexity of the non-binary row-ISI detector. For $L \times L$ characterized channel, the row-ISI trellis consists of $2^{L(L-1)}$ states. Therefore, this detector becomes infeasible for $L > 3$.

IV. Simulation Results and Analysis

Traditionally, BER is measured as a function of signal-to-noise (SNR) ratio. As TDMR is one of the potential next-generation magnetic recording systems, we are interested in estimating the operating channel density of the TDMR system that maximizes the user storage capacity. Although, the SNR is related to the channel density that relationship varies with the SNR definition and is not consistent across the board. In this work, we determine the BER performance of various detectors directly as a function of channel density.

For our simulations, we characterized the channel as a 3×3 matrix and assumed a 2D Gaussian profile for the head response with a T50 of 1 grain diameter, where the grain diameter is defined as the square root of the average grain size. This is a sharper response than what is currently achievable, but represents a speculated value for a future recording system and can be modified when the number becomes known. The results are as shown in Figure 5. The horizontal axis is the bit cell size normalized to the average grain size or (channel density)$^{-1}$. The channel density is varied by changing the size of the bit cell. As the normalized bit size increases the SNR improves and the BER drops for all detectors. Since we assume a BAR of 2, the ITI turns out to be significantly smaller than the ISI. Consequently, the 1-D MAP detector, which doesn't account for the ITI performs fairly close to the 2-D MAP detector, while the separable 2-D MAP detector performs even closer. It is interesting to note that the inversion detector performs marginally better than other detectors at high densities, but does worse as the density drops.

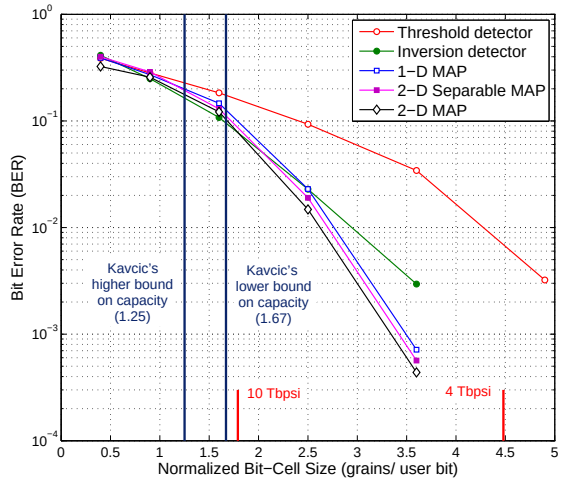

Fig. 5. BER performance of various detectors at different channel densities, when T50 = 1 grain diameter.

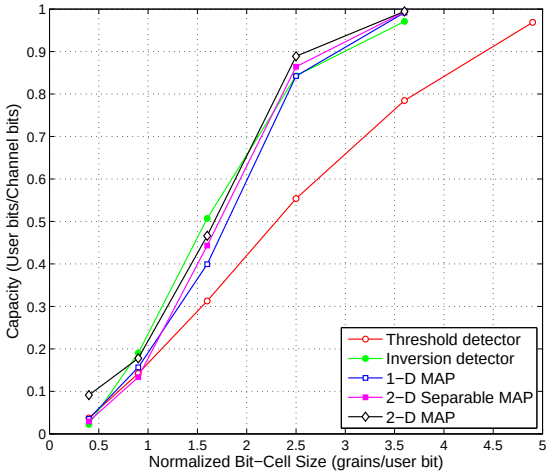

Fig. 7. The channel capacity assuming a BSC channel with probability of error p =BER.

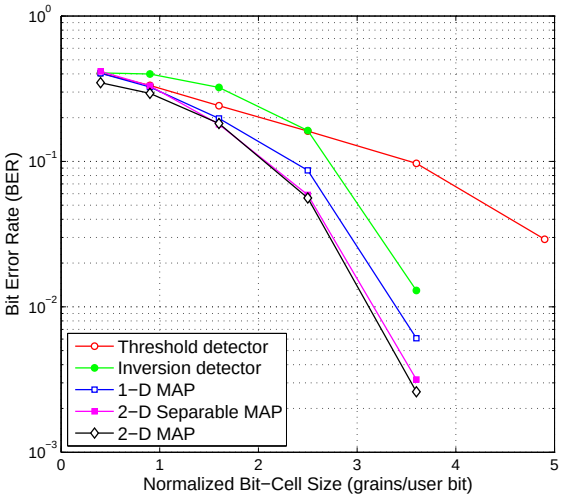

Fig. 6. BER performance of various detectors at different channel densities, when T50 = 1.8 grain diameter

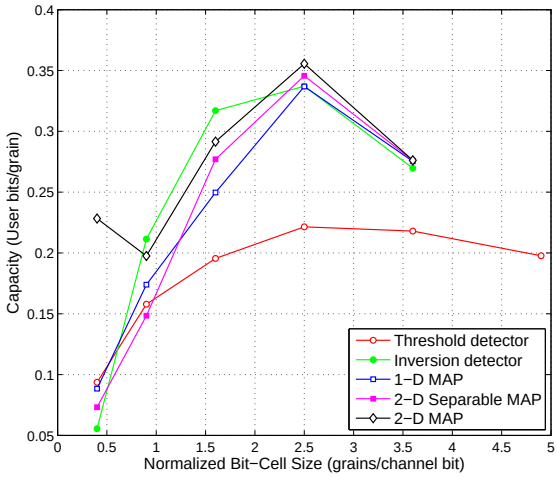

Fig. 8. Lower bound on TDMR channel capacity in terms of user bits per grain.

As the T50 of the response is increased, the 2-D MAP detector and 2-D separable MAP detector start to outperform the 1-D MAP detector by a larger margin as the ITI becomes more significant at all densities. This result is shown in Figure 6, where T50 is 1.8 times the average grain diameter.

The capacity [14] for a binary symmetric channel (BSC) can be calculated according to $C = 1 + p\log_2(p) + (1-p)\log_2(1-p)$ where p is the probability of error over the BSC: $p = P(1/0) = P(0/1)$. Figure 7 shows the capacities for each detector, if the combined channel+detector system behaved like a BSC with probability of error p =BER. C has the same units as the code rate R, in user bits per channel bits. According to Shannon's theorem [14], the channel capacity C is the theoretical limit of the best code rate that can operate over the BSC with error-free transmission. This means that no code exists over the channel, with rate larger than C, that can achieve error-free transmission. Conversely, and equally importantly, codes *do* exist with code rates $R < C$ that can produce error-free transmission, i.e. the error rate can be brought arbitrarily low. These joint conclusions mean that finding the actual capacity of the granular media channel is very important. Unfortunately, this is also very difficult to do.

In [15], Kavcic et. al. have bounded the channel capacity for a granular medium channel under the assumption of a medium with just 4 types of grains, and without ISI/ITI/AWGN. The bounds computed there place the capacity between $0.6 < C < 0.8$ bits per grain (bpg), these bounds are shown on the horizontal axis in Figure 5. Also marked on the horizontal axis are the 10Tb/in^2 and 4 Tb/in^2 points assuming an average grain-size of 6nm.

It should be noted that Shannon's theorem needs to be

interpreted with a some caution. Firstly, it is an existence theorem, in that it guarantees the existence of a code with rate $R < C$ that can produce error-free transmission, but it does not tell us how to construct such a code. Secondly, codes that approach the Shannon capacity will have block lengths that tend to ∞, and the corresponding computational complexities to decode them as well. Hence codes operating at capacity are not practical. The challenge becomes to find codes that approach the capacity, while remaining "practical". In 1-D, LDPC codes are known to be practical codes that come very close to the Shannon capacity limit.

Another quantity of interest is the limit on the achievable user density, that can be obtained by dividing the channel capacity plots in Figure 7 (user bits/channel bit) by the normalized bit cell size (in grains per channel bit) and has the unit of user bits per grain. This gives the plots shown in Figure 8. Note that the horizontal axis now refers to the normalized *channel* bit cell size. This figure shows that the storage capacity peaks at 0.36 user bits per grain (bpg) for the 2D-MAP detector, when operating at a channel density of 0.4 channel bpg. To be explicit the best performance amongst the tested detectors, is the 2D-MAP detector operating at a user bit density of 0.4 channel bits per grains, having a raw BER of about 1.5×10^{-2} and an equivalent raw BSC capacity of almost 0.9 user bits/channel bit. If we could find a code that operated at the BSC capacity of 0.9 user bits/channel bit, it would have the corresponding user bit density of 0.36 user bits per grain.

As mentioned, [15] showed that the lower and upper bounds on capacity are 0.6 and 0.8 user bpg, assuming a slightly more idealistic medium. We can perhaps optimistically target the lower bound of the density at 0.6 user bpg, given that our channel model has arbitrary grain sizes and ISI/ITI as well as AWGN. The BSC capacity of 0.36 user bits/grain for the 2D-MAP detector still falls quite short of this target. This gap can be attributed to the suboptimality of the 2D-MAP detector. The 2D-MAP is optimal when the noise is white. However it is known from the 1D case that the media noise is quite far from white, and strongly signal dependent. To close the gap between the existing detectors, and the targeted channel density of 0.5 user bpg, we need to implement more powerful detectors that take into account the colored and signal dependent noise. Once this is done, it is possible that the operating point may shift from channel density of 0.4 bpg.

This method of plotting BER as a function of channel density allows a direct comparison of the maximum achievable density and the density achieved by a particular detector and decoder. From Shannon's theorem, we know that no code exists that can achieve error-free transmission at (rates) densities larger than capacity, and conversely, codes do exist that can achieve error-free transmission at (rates) densities below capacity. In Figure 5, this means that once codes are introduced, the FER will necessarily be large to the left of the Kavcic capacity line (lower bound), and will have the possibility to fall off quickly, to the right of the capacity line, the goal being to find the code that pushes the limits of the capacity while remaining computationally tractable. The proximity of the 10Tb/in^2 line to the lower bound means that it is going to be very difficult to find a code that has a waterfall region that can drop down to the 10^{-14} error rate levels required for commercial viability in the gap between Kavcic's lower bound and the 10Tb/in^2 mark (assuming a grain size of 6nm). This means that 10Tb/in^2 is not likely to be achievable on media with 6nm grains, in any situation (which may also have applications in HAMR). By contrast, 4Tb/in^2 looks quite feasible, the challenge remains to find and test the code that has a sharp drop off, that occurs to the left of the 4Tb/in^2 mark on the graph.

V. Conclusion

The novel contributions of this work are threefold. We have proposed and characterized a novel model, the GFP, for the TDMR channel based on Voronoi grains and micromagnetic simulations. We have implemented and tested 3 detectors over the previous TDMR channel model, and we have presented a new way of plotting and interpreting the results as a function of the user bit density.

The new channel model benefits from the best of 2 worlds, having the speed required to produce billions of bits for channel simulations, while having the accuracy of micromagnetic simulations. It requires a characterization phase lasting possibly days to populate the LUT. The future work for this model is to test the GFP with some of the detectors described in this paper.

The detectors implemented here were taken from the literature, but to our knowledge have not previously been applied to a TDMR channel. Based on BSC capacities calculated using these detectors, and capacity results obtained from [15] we are able to estimate how far from capacity these detectors are performing. We are hypothesizing that the coloured media noise is the main cause of the gap between the current detectors' performance and capacity. Thus the future work for the detectors is to implement noise predictive (NP) and pattern dependent noise predictive (PDNP) versions of the current detectors to close this gap.

In the past, BER/FER performance plots have typically been as a function of the SNR, since the SNR is expected to degrade with increasing density. This method suffers from too many individual definitions of SNR on the one hand, and a lack of a link to a study showing how the SNRs degrades with density on the other. In order to draw stronger conclusions, it is advantageous to plot the BER/FER performance curves directly as a function of the density. This can only be done with an appropriate channel model that takes the density into account. Our plots are tied to the channel model using Voronoi cells to mimic the behaviour of the grains, and the density is defined with respect to the average grain size. With user bit sizes plotted on the horizontal axis, the benefits are 3-fold. First, the performance of the detectors can be directly compared with the results from capacity computations giving a quantitative estimate of how well the detectors are performing. Second, the absolute density can be plotted on the same axis for a given grain size giving an estimate of how close the density is to capacity and therefore whether or not that density is likely to be achievable. Third, once codes are introduced, a

water-fall region is again expected as with the BER vs SNR plots. The success or failure of TDMR at a given density can be partially claimed by observing whether the waterfall region occurs above or below the targeted density. Only a partial success can be claimed because we are neglecting the effect of error floors that may occur below the field of view. In the absence of the error floors, and if the channel model is accurate, then the plots introduced in this paper, can be used to determine the viabilty of TDMR as an architecture to support towards 10Tb/in^2 recording.

The authors would like to acknowledge Roger Wood as the proposer of TDMR and the motivator behind its continued progress. This work was sponsored by INSIC.

REFERENCES

[1] R. Wood, M. Williams, A. Kavcic, and J. Miles, "The feasibility of magnetic recording at 10Tb/in^2 on conventional media," *IEEE Trans. Magn.*, vol. 45, pp. 917–923, Feb. 2009.

[2] H. J. Richter, "The transition from longitudinal to perpendicular recording," *J. Phys. D: Appl. Phys*, pp. R149–R177, Apr. 2007.

[3] S. N. Piramanayagam and K. Srinivasan, "Recording media research for future hard disk drives," *J. Magnetism and Magnetic Materials*, pp. 485–494, May 2008.

[4] H. Richter, A. Dobin, O. Heinonen, K. Gao, R. Veerdonk, R. Lynch, J. Xue, D. Weller, P. Asselin, M. Erden, and R. Brockie, "Recording on bit-patterned media at densities of 1 Tb/in^2 and beyond," *IEEE Trans. Magn.*, vol. 42, no. 10, pp. 2255–2260, Oct. 2006.

[5] R. E. Rottmayer, S. Batra, D. Buechel, W. A. Challener, J. Hohlfeld, Y. Kubota, L. Li, B. Lu, C. Mihalcea, K. Mountfield, K. Pelhos, C. Peng, T. Rausch, M. A. Seigler, D. Weller, and X. Yang, "Heat assisted magnetic recording," *IEEE Trans. Magn.*, vol. 42, pp. 2417–2421, Oct. 2007.

[6] J.-G. Zhu, X. Zhu, and Y. Tang, "Microwave assisted magnetic recording," *IEEE Trans. Magn.*, vol. 44, no. 1, pp. 125–131, Jan. 2008.

[7] K. S. Chan, J. Miles, E. Hwang, B. V. K. Vijayakumar, J. G. Zhu, W. C. Lin, and R. Negi, "TDMR platform simulations and experiments," *IEEE Trans. Magn.*, 2009, accepted for publication.

[8] P. Kasiraj and M. Williams, "System and method for writing HDD depending on head skew," 2005, U.S. Patent 6,967,810 B2.

[9] J. Miles, D. McKirdy, R. Chantrell, and R. Woods, "Parametric optimization for terabit perpendicular recording," *IEEE Trans. Magn.*, vol. 39, pp. 1876–1890, July 2003.

[10] B. M. Kurkoski, "Towards efficient detection of two-dimensional intersymbol interference channels," *IEICE Trans. on. Fundamentals*, vol. E91-A, no. 10, Oct. 2008.

[11] A. Krishnan, R. Radhakrishnan, and B. Vasić, "Ldpc decoding strategies for two-dimensional magnetic recording," in *Proc. IEEE Global Telecommunications Conference (GLOBECOM)*, Honolulu, Hawaii, Dec. 2009, accepted for publication.

[12] L. C. Barbosa, "Simultaneous detection of readback signals from interfering magnetic recording tracks using array heads," *IEEE Trans. Magn.*, vol. 26, no. 5, Sept. 1990.

[13] Y. Wu, J. A. O'Sullivan, N. Singla, and R. S. Indeck, "Iterative detection and decoding for separable two-dimensional intersymbol intereference," *IEEE Trans. Magn.*, vol. 39, no. 4, July 2003.

[14] C. E. Shannon, "A mathematical theory of communications," *Bell Syst. tech J.*, p. 379, 1948.

[15] A. Kavcic, B. Vasic, W. Ryan, and F. M. Erden, "Channel modeling and capacity bounds for two dimensional magnetic recording," 2009, digest accepted for TMRC 2009.